PROCEEDINGS OF SPIE

SPIEDigitalLibrary.org/conference-proceedings-of-spie

Passively Q-switched Nd:YVO4 laser operating at 914 nm

Naegele, Marco, Stoppel, Klaus, Ridderbusch, Heiko, Dekorsy, Thomas

Marco Naegele, Klaus Stoppel, Heiko Ridderbusch, Thomas Dekorsy, "Passively Q-switched Nd:YVO4 laser operating at 914 nm," Proc. SPIE 11259, Solid State Lasers XXIX: Technology and Devices, 112590P (21 February 2020); doi: 10.1117/12.2543777

SPIE.

Event: SPIE LASE, 2020, San Francisco, California, United States

Downloaded From: https://www.spiedigitallibrary.org/conference-proceedings-of-spie on 05 Oct 2020 Terms of Use: https://www.spiedigitallibrary.org/terms-of-use

Passively Q-switched Nd:YVO_4 Laser operating at 914 nm

Marco Naegele[a,b], Klaus Stoppel[a], Heiko Ridderbusch[a], and Thomas Dekorsy[b,c]

[a] Robert Bosch GmbH, Chassis Systems Control, Abstatt, Germany;
[b] Institute of Aerospace Thermodynamics, University of Stuttgart, Germany;
[c] Institute of Technical Physics, German Aerospace Center (DLR), Stuttgart, Germany;

ABSTRACT

A diode-pumped passively Q-switched Nd:YVO_4 laser operating at 914 nm is demonstrated. The solid-state laser is quasi-continuously pumped at 808 nm using a 35 W fiber-coupled diode laser. Several Cr^{4+}:YAG saturable absorbers with different outcoupling coefficients are utilized to optimize the overall system performance. The simple two component cavity design reduces the system complexity and enables efficient pump power conversion along with long-term stability concerning power and wavelength. Furthermore, temperature dependent stimulated-emission cross-section in the Q-switched regime is investigated by observing the evolution of the single pulse energy over a temperature range of 70 K.

Keywords: Laser crystals, Laser energy measurements, Laser systems engineering, Neodymium, Optical pumping, Pulsed laser operation, Q switched lasers, Q switching, Resonators, Solid state lasers

1. INTRODUCTION

Diode-pumped passively Q-switched solid-state lasers are a compact, efficient, and simple way to generate high peak power pulses in the nanosecond regime. Such lasers operating in the near infrared region have wide applications in the fields of sensor industry, medical treatment, scientific research, and defense.
Beside the commonly utilized spectral transitions at 1064 nm and 1342 nm, Nd-doped gain media offer a $^4F_{3/2} \rightarrow {}^4I_{9/2}$ transition at around 900 nm with quasi-three-level laser character.
Laser operation around 900 nm is interesting for a large variety of applications and thus has been intensively investigated in the past years.
As an example, frequency doubling of 900 nm photons via second-harmonic generation offers blue laser light which is especially interesting for underwater communication, display technology, and optical data storage.[1,2]
Furthermore, laser light around 900 nm is beneficial for efficiently pumping of Yb-doped lasers operating at 980 nm with low quantum defect[3,4] or remote sensing in water-vapor lidars and differential-absorption lidars (DIAL).[5]
Despite all promising applications and high demand, operation of Nd-doped as quasi-three level is challenging compared to the four-level operation at 1064 nm. As the lower laser level is a upper ground state manifold high thermal population leads to significant reabsorption at 914 nm.[6] This effect was firstly considered by T.Y. Fan and R.L. Byer[7] and investigated by W.P. Risk in 1988.[8]
Additionally to the effect of reabsorption, stimulated-emission cross-section at 914 nm is roughly 30-times smaller compared to 1064 nm which increases the operation threshold and additionally necessitates high losses for the four-level transition.[9] If the induced losses at 1064 nm are to small, dual-wavelength operation is observed[10] or the laser is not operating at the quasi-three level transition at all.
The first quasi-three level Nd:YAG laser was realized by T.Y. Fan and R.L. Byer in 1987.[7] Without a doubt, today Nd:YAG is the most popular laser crystal among Nd-doped materials. Compared to Nd:YAG the commonly used Nd:YVO_4 offers significant advantages such as a larger stimulated-emission cross-section and linearly polarized laser output due to birefringence instead of losses induced by depolarization.[11] Additionally, Nd:YVO_4 offers broader and especially higher absorption coefficients at 808 nm and 880 nm which have been observed by T. Taira[12] and Y. Sato in the past.[13] Considering fluorescence lifetime in pulsed laser operation, Nd:YAG has a lifetime of roughly 230 µs and is favored for application with higher pulse energies, while Nd:YVO with a shorter lifetime of around 100 µs clearly fulfills requirements of increased repetition rates. Although YAG has a

Further author information: marco.naegele@de.bosch.com

Solid State Lasers XXIX: Technology and Devices, edited by W. Andrew Clarkson, Ramesh K. Shori, Proc. of SPIE Vol. 11259, 112590P · © 2020 SPIE
CCC code: 0277-786X/20/$21 · doi: 10.1117/12.2543777

Downloaded From: https://www.spiedigitallibrary.org/conference-proceedings-of-spie on 05 Oct 2020
Terms of Use: https://www.spiedigitallibrary.org/terms-of-use

better thermal conductivity in general, Y. Sato has shown in 2006 that conductivity of Nd:YVO can be quite comparable.[14]
In the past decades, a lot of research on Nd:YVO_4 operating at 1064 nm was performed. In 2000, P. Zeller and P. Peuser demonstrated a continuous-wave (cw) Nd:YVO laser with a slope efficiency of 22.8 % related to an output power of 3 W. To date, Nd:YVO lasers operated in cw with the highest conversion efficiency of 33.4 % which was obtained under double-end polarized pumping by P. Jiang in 2016.[11]
Due to the above mentioned difficulties in quasi-three level operation, only few results for passively Q-switched Nd:YVO lasers have been published. In 2012, X. Yu et al. demonstrated a high power passively Q-switched Nd:YVO_4/Cr^{4+}:YAG laser with nanosecond pulses and repetition rates of up to 2 MHz linked to a conversion efficiency of 14.9 %.[18]
Within the framework of this work, further investigations towards efficient passively Q-switched Nd:YVO lasers operating at 914 nm are revealed and system properties characterized.

2. EXPERIMENTAL SETUP

The experimental setup is schematically shown in the left part of Figure 1. A fiber-coupled semiconductor pump laser with 35 W output power is temperature controlled via water cooling. Temperature of the laser is adjusted to meet the wavelength of the maximum absorption in Nd:YVO_4 at around 808 nm. A 25 mm plano-convex spherical lens collimates the divergent pump beam before it passes a half-wave plate where the polarization is rotated in order to compensate for the anisotropic crystal structure and absorption properties in Nd:YVO_4.[15] Another spherical lens with 37 mm focal length focuses the pump to a spot size of approximately 200 µm ($1/e^2$ waist).
The cavity consists of a 0.2 at% doped Nd:YVO_4 (3x3x5 mm^3) crystal and a Cr:YAG saturable absorber with 96 % initial transmission. All facets have an antireflection coating at 808 nm and 1064 nm while the oscillator at 914 nm is constructed via an incoupling high reflective (HR) and an outcoupling partial reflective (PR) coating with an optional outcoupling reflectivity of 91 % and 95 %, respectively. The outcoupling mirror is directly coated onto the absorber via dielectric coating. Both crystals, Nd:YVO_4 and Cr^{4+}:YAG, are temperature stabilized at 20 °C.

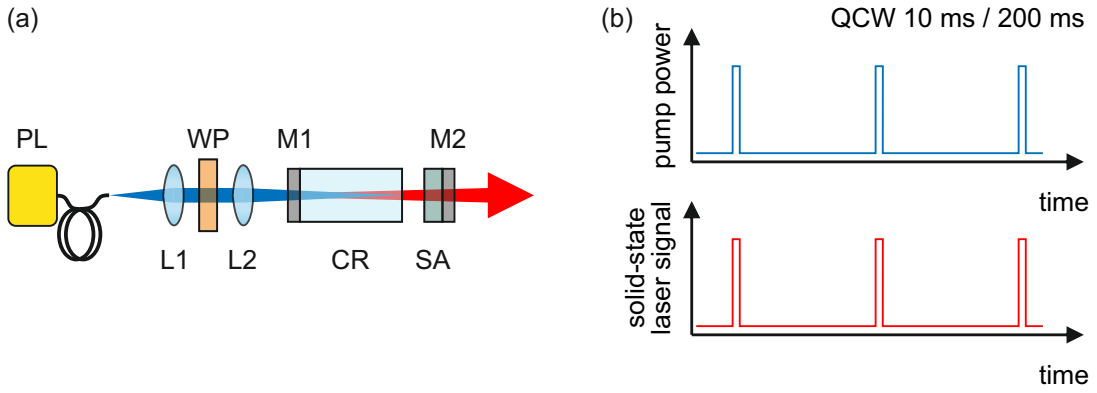

Figure 1. (a) Optical setup of the solid-state laser pumped by a diode-coupled semiconductor pump laser. Abbreviations: L: lens; WP: half-wave plate; M: mirror; CR: Nd:YVO_4 laser crystal; PL: pump laser; SA: Cr:YAG saturable absorber. (b) QCW pumping scheme with 5 % duty cycle (10 ms/200 ms) and resulting solid-state laser pulse train.

In all experiments shown here, a 10 ms/200 ms quasi-continuous-wave (QCW) pumping scheme related to 5 % duty cycle is applied. The right part of Figure 1 illustrates this relationship schematically along with generated solid-state laser signal resulting from QCW pumping.
Today, QCW pumping is used for many applications such as light detection and ranging (LiDAR) systems or industrial micro-material processes. In general, pumping with a low duty cycle is beneficial with respect to thermal crystal load and associated instabilities.

Downloaded From: https://www.spiedigitallibrary.org/conference-proceedings-of-spie on 05 Oct 2020
Terms of Use: https://www.spiedigitallibrary.org/terms-of-use

3. EXPERIMENTAL RESULTS

The outcoupled solid-state laser pulse train (91 % output coupling reflectivity) is measured with a fast 5 GHz InGaAs photodiode (Thorlabs, rise time: 70 ps, fall time 110 ps) and a 4 GHz oscilloscope (Teledyne LeCroy, HDO9404). Figure 2 shows the temporal output characteristics at an applied QCW pump power of 200 mW which results in an pulse train with 19.79 kHz. Subfigure 2(a) shows part of the detected train within a range of 2 ms possessing an excellent peak to peak stability of 1.2 %. The corresponding repetition rate evolution is shown in Fig. 2(b) with a temporal jitter of only 1 %. An exemplary single pulse at around 5.0823 ms of the above pulse train is depicted in Fig. 2(c). Applying a Gaussian fit results in a FWHM of 10.53 ns. The pulse exhibits an asymmetric profile with a steeper leading edge and a sustained tail. Asymmetric temporal pulse shapes are common for Q-switched lasers and have been experimentally and theoretically analyzed in the past.[16,17] Subfig. 2(d) shows the according temporal pulse width advancement owing a mean pulse duration of 10.57 ns and a standard deviation of 0.01 %.

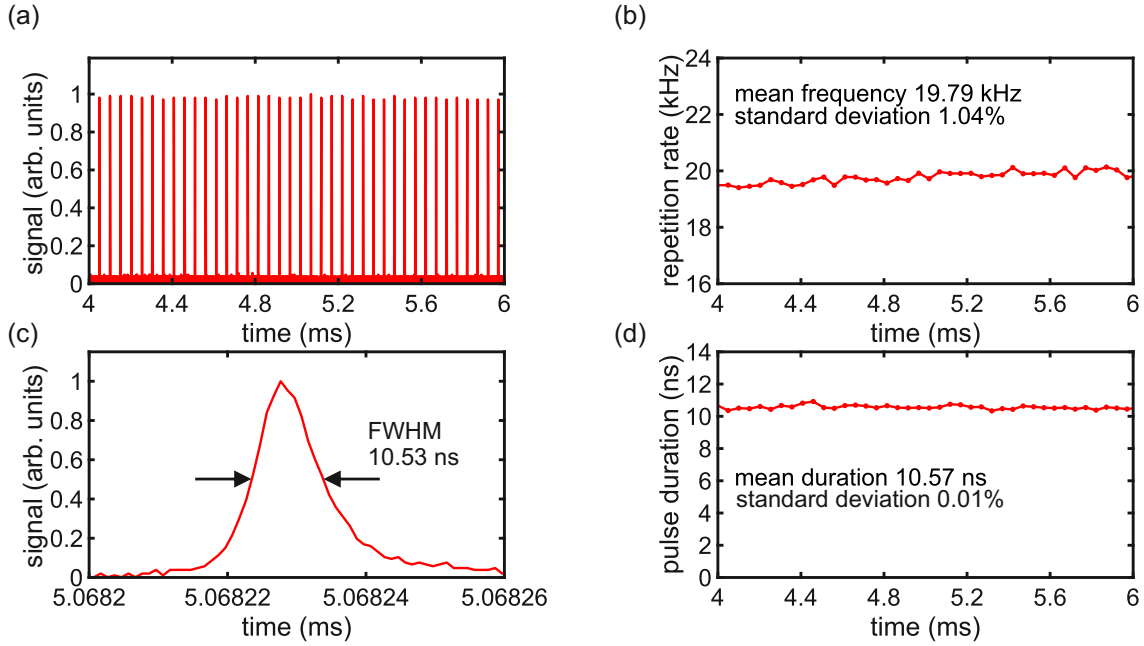

Figure 2. Temporal pulse train characteristics are recorded at a QCW pump power of 200 mW for an outcoupling reflectivity of 91 %. (a) Zoom in of the measured pulse train with a peak to peak standard deviation of 1.2 % over a range of 2 ms. (b) shows repetition rate evolution at a mean frequency of 19.79 kHz with temporal jitter of only 1.04 %. A single pulse with 10.53 ns FWHM is shown in (c), while (d) depicts evolution of the resulting evaluated single pulse duration over the whole 2 ms range. A mean pulse duration of 10.57 ns with 0.01 % standard deviation are obtained.

Two different outcoupling reflectivities at 914 nm (R 91 % and R 95 %) are used to characterize the pump power dependent laser output. Figure 3(a) shows average output power for an increasing QCW average pump power of up to 1200 mW. Initially, the output power is increasing linearly for both reflectivities and tends to saturate for higher pump powers. A maximum average output power of 205 mW (1200 mW pump power) and 114 mW (900 mW pump power) is achieved for R91 % and R95 %, respectively. A maximum optical to optical conversion efficiency of 20.2 % is obtained for an reflectivity of 91 %, which is to the best of our knowledge, the highest conversion efficiency achieved with Q-switched Nd:YVO_4 operated in the quasi-three level regime and around 10 % higher than the results obtained in 2012 by X. Yu.[18]
The temporal pulse length (FWHM) is not changing significantly over the whole pump power range and fluctuates for both outcoupling coatings around a value of 11 ns. On the other hand, the pulse repetition rate increases, as expected, approximately linearly with higher pump power. It is remarkable that both repetition rates start

Downloaded From: https://www.spiedigitallibrary.org/conference-proceedings-of-spie on 05 Oct 2020
Terms of Use: https://www.spiedigitallibrary.org/terms-of-use

to decrease for higher applied pump powers. This effect has already been observed in previous publications by M. Wei[19,20] where its occurrence is attributed to nonlinear dynamics which induce chaotic pulse train patterns and satellite pulses. Experimental investigations aside from the results shown in this publication are in great accordance to the results obtained by Wei et al.. The maximum achieved repetition rate of both systems is 123 kHz and 83 kHz for R91 % and R95 %, respectively. As there is less of the intracavity power coupled out for a reflectivity of 95 % the nonlinear dynamics arise at a lower pump power compared to R91 % as the remaining intracavity power is higher.

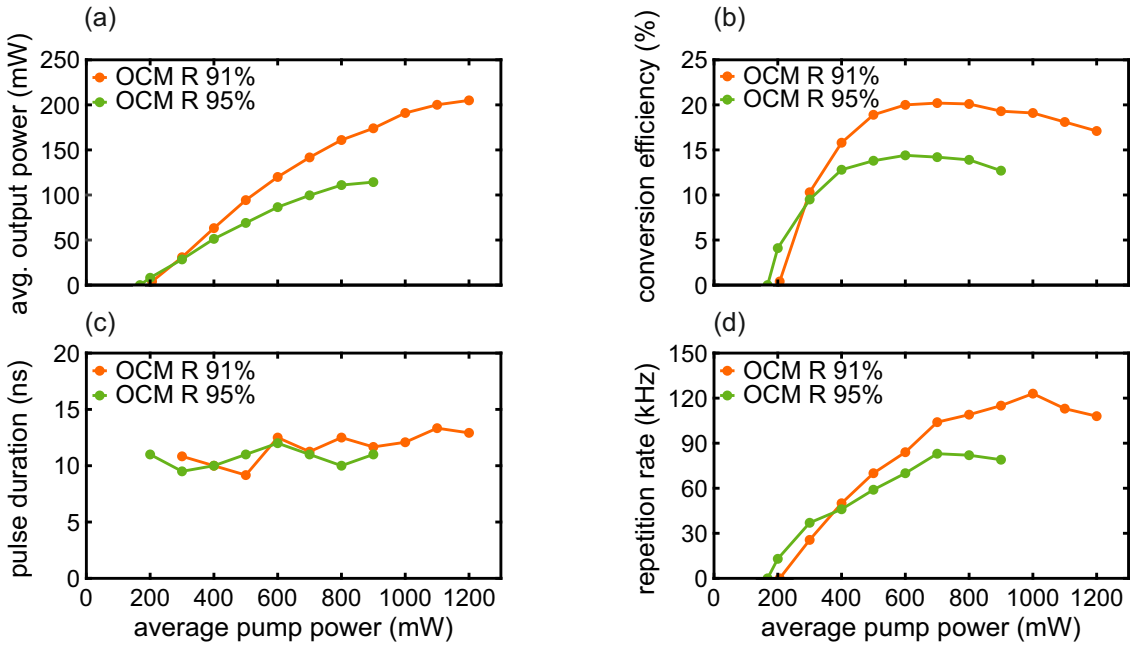

Figure 3. Output characteristics for both outcoupling reflectivities (OCM R91 % and R95 %) as a function of applied QCW pump power. For both reflectivites, the output power increases linearly once the threshold is reached and tends to saturate for higher pump powers (a). A maximum optical conversion efficiency of more than 20 % is achieved in (b) for an outcoupling reflectivity of 91 %. In (c), the temporal pulse length does not change significantly with different applied pump powers of 1200 mW and 900 mW, respectively. Repetition rate evolution with a clear maximum and decreasing rates for both OCM reflectivities according to nonlinear dynamics, are depicted in (d).

Stimulated-emission cross-section of the gain media strongly influences laser operation. A small stimulated-emission cross-section results in high laser operation threshold.[21] Furthermore, the maximum spectral amplification and thus laser operation wavelength is dependent on the peak of this quantity.[22] As temperature has significant influence on the stimulated-emission cross-section in Nd-doped materials, several publications already obtained the dependency on temperature at 1064 nm.[23,24] In 2016, G. Krishnan[25] measured the temperature influence at 914 nm by detecting fluorescent radiation and using the Füchtbauer–Ladenburg relation.[26] In contrast to that publication, within the framework of this paper, a different technique is applied in order to determine temperature dependency.
In theory the pulse energy of a passively Q-switched can be derived to

$$E_\mathrm{p} = \frac{\mathrm{h}\nu A}{2\gamma} \cdot \ln\left(\frac{1}{R}\right) \cdot \ln\left(\frac{n_\mathrm{i}}{n_\mathrm{f}}\right) \cdot \frac{1}{\sigma(T)} \tag{1}$$

with Planck's constant h, photon frequency ν, area of the gain medium A, inversion reduction factor γ ($\gamma = 2$ for a three-level system), reflectivity of the resonator output coupler R, initial population inversion n_i, final population inversion n_f and temperature dependent stimulated-emission cross-section $\sigma(T)$.[27]

Downloaded From: https://www.spiedigitallibrary.org/conference-proceedings-of-spie on 05 Oct 2020
Terms of Use: https://www.spiedigitallibrary.org/terms-of-use

Derivation of the pulse energy E_p to temperature T results in

$$\frac{\mathrm{d}E_\mathrm{p}}{\mathrm{d}T} = E_\mathrm{p}(-\frac{1}{\sigma}\frac{\mathrm{d}\sigma(T)}{\mathrm{d}T}) \tag{2}$$

which can be further transformed into

$$\sigma(T) = \frac{E_0 \cdot \sigma_0}{\frac{\mathrm{d}E_\mathrm{p}}{\mathrm{d}T}T + E_0}, \tag{3}$$

where σ_0 is the temperature independent cross-section ($4.8 \times 10^{-20}\,\mathrm{cm}^2$) according to Chen et al.[6] Figure 4(a) shows the experimentally recorded relation between single pulse energy and temperature of the Nd:YVO_4 crystal measured from 15 °C to 85 °C. A linear fit determines the slope m and intersection value b. According to Eq. (3), the fitted slope and intersection can be utilized to the calculate stimulated-emission cross-section as a function of temperature. The relation between this cross-section and temperature is shown in Figure 4(b). Using a linear fit, the stimulated-emission cross-section decreases with a negative slope of $9.8 \times 10^{-23}\,\mathrm{cm}^2\,\mathrm{K}^{-1}$. This is in good accordance to the temperature dependency observed by Krishnan et al.[25] ($-1.39 \times 10^{-22}\,\mathrm{cm}^2\,°\mathrm{C}^{-1}$), while taking different crystal doping concentrations and measurement techniques into account.

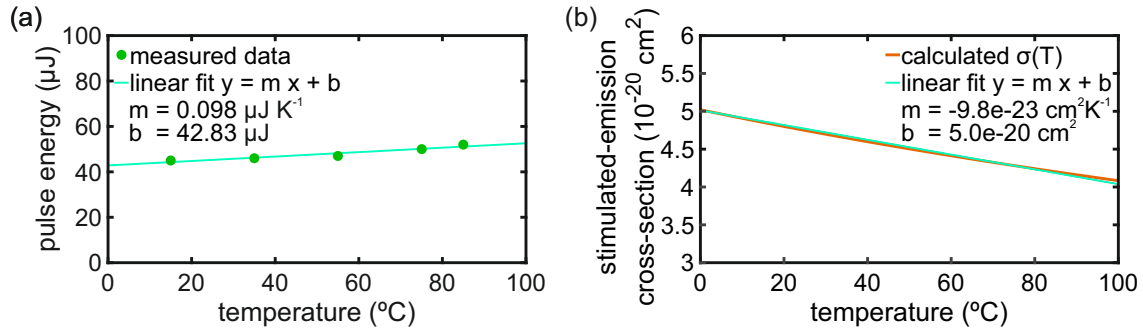

Figure 4. Derivation of the stimulated-emission cross-section dependency on temperature according to single pulse energy measurement. The obtained single pulse energy as a function of crystal temperature is recorded between 15 °C and 85 °C (a). Linear development of stimulated-emission cross-section as a function of temperature results in a negative slope of $9.8 \times 10^{-23}\,\mathrm{cm}^2\,\mathrm{K}^{-1}$ in (b).

In the following, all experimental results are related to an outcoupling reflectivity of 91 %. Long-term stability measurements for 60 min are performed to compare pump laser and solid-state laser in terms of normalized average output power, central wavelength and FWHM. A non-polarizing beam splitter enables simultaneous measurement of pump laser and solid-state laser power with two OPHIR 3A-P thermal power measurement sensors. Normalized average output power fluctuations of 0.14 % and 0.65 % are observed for the pump laser and solid-state laser in Figure 5. Small fluctuations of the solid-state laser seem superimposed with a coarse periodic fluctuation pattern showing a periodicity of roughly 10 min. While occurrence of small fluctuations might be linked to thermal lens related instabilities and longitudinal mode competition, a reason for coarse periodic deviation is not understood yet. Although coarse fluctuations add a substantial contribution to power fluctuation, a standard deviation far below 1 % is an excellent result. Spectral evolution of both lasers is recorded using an Ocean Optics HR4000 spectrometer (sampling rate 1 Hz, 5 µm slit, 699 nm-1126 nm, 0.24 nm resolution) and analyzed in Matlab using a Gaussian fit function providing FWHM and central wavelength. Both systems show small central wavelength fluctuation of only 0.005 nm and 0.03 nm, respectively. It is important to note that due to the low spectrometer resolution of only 0.24 nm small fluctuations and distinction between adjacent longitudinal modes is not possible. With a cavity length of only around 8 mm spacing between adjacent modes is estimated to be on the order of 30 pm. The same applies for spectral bandwidth measurements shown at the bottom of Figure 5. Hereby, improved central wavelength stability of the solid-state laser compared to a semiconductor counterpart can be explained by the lower temperature of changes of involved energy levels in the solid state systems compared to semiconductors.

Downloaded From: https://www.spiedigitallibrary.org/conference-proceedings-of-spie on 05 Oct 2020
Terms of Use: https://www.spiedigitallibrary.org/terms-of-use

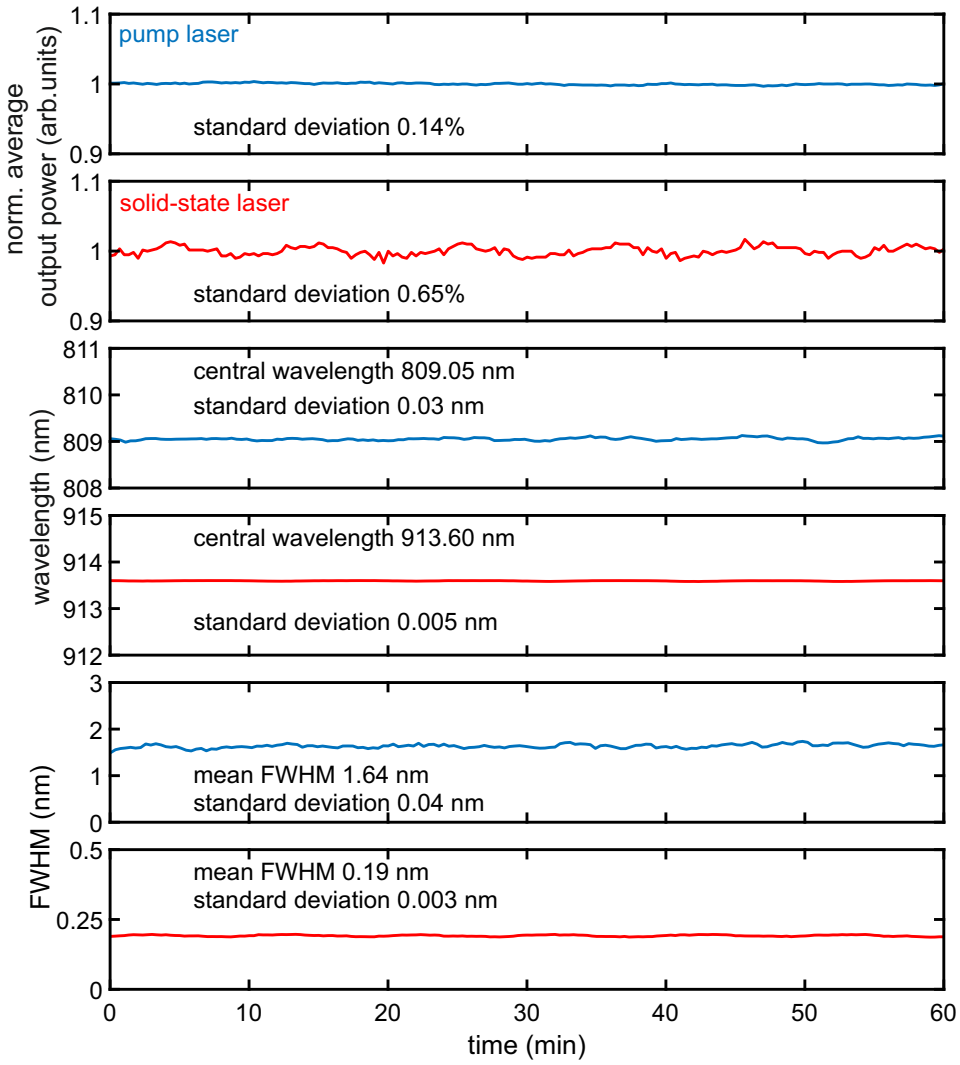

Figure 5. Simultaneously long term average output power, central wavelength and spectral bandwidth measurement of both, pump laser and solid-state laser, respectively. A non-polarizing beam splitter enables record of pump laser fluctuation and solid-state laser fluctuations for an applied pump power of 500 mW at the same time. Average output power of the solid-state laser reaches a stability of 0.65 % standard deviation. Both, the central frequency fluctuation (fit evaluation 5 pm) and the corresponding bandwidth variation (fit evaluation 3 pm) exhibits a spectrometer resolution limited deviation below 240 pm.

Laser beam analysis is performed using an Ophir $M^2 - 200s$ instrument with an externally triggered input signal. Figure 6 depicts beam evolution after propagation through 400 mm NIR lens at an applied pump power of 500 mW. In both direction, an $M^2 < 1.1$ is obtained indicating an almost diffracted-limited beam. The inset shows a typical transverse beam profile recorded at 500 mm indicating a fundamental transverse Gaussian intensity distribution which is in good accordance to the diffraction-limited beam. Beside beam propagation factor M^2, beam quality measurements in general provide useful information about inherent laser properties as beam waist, Rayleigh-length and far-field divergence. By means of these parameters conclusion on further system design optimization can be drawn. A calculated Rayleigh-length of 180 mm and an intracavity laser beam waist of around 230 µm indicates reasonable choice of crystal length and pump focal length.

Downloaded From: https://www.spiedigitallibrary.org/conference-proceedings-of-spie on 05 Oct 2020
Terms of Use: https://www.spiedigitallibrary.org/terms-of-use

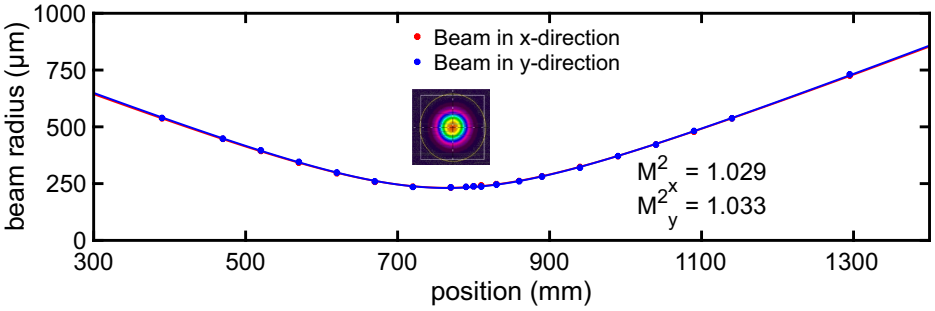

Figure 6. Beam quality factor measurement in x and y direction at an applied pump power of 500 mW. Both beam directions are almost diffraction-limited with an M^2 close to one. The inset depicts a transversal intensity profile recorded at a measurement position of 500 mm.

4. CONCLUSION

In conclusion, we have presented an highly efficient Q-switched 914 nm laser consisting of a compact and simple cavity design. Using a QCW pumping scheme with 5 % duty cycle (10 ms/200 ms), a maximum optical-optical conversion efficiency of more than 20 % has been obtained which is an excellent value especially with respect to a pulsed quasi-three level laser. The high conversion efficiency along with a small quantum defect (808 nm→914 nm) is in particular especially interesting for a wide range of applications with respect to thermal management. Furthermore, an overall great system stability is obtained with stable pulse trains as well as small output power and spectral fluctuation.

Measuring the single pulse energy increase within a temperature range of 70 °C has provided a value for stimulated-emission cross-section as a function of temperature.

Future ideas, include further setup simplification by employing a monolithic cavity design and additional investigation of system limits especially with respect to nonlinear dynamics. Numerical simulations based on rate equations including reabsorption effects and thermal population additionally help to optimize system parameter and define operation limits.

REFERENCES

1. T. J. Kane, G. Keaton, M. A. Arbore, D. R. Balsley, J. F. Black, J. L. Brooks, M. Byer, L. A. Eyres, M. Leonardo, J. J. Morehead, *et al.*, "3-watt blue source based on 914-nm Nd:YVO_4 passively-Q-switched laser amplified in cladding-pumped Nd:fiber," in *Advanced Solid-State Photonics*, p. 160, Optical Society of America, 2004.
2. S. Bjurshagen, D. Evekull, and R. Koch, "Efficient generation of blue light by frequency doubling of a Nd:YAG laser operating on $4^F_{3/2} - 4^I_{9/2}$ transitions," *Applied Physics B* **76**(2), pp. 135–141, 2003.
3. J. Koerner, C. Vorholt, H. Liebetrau, M. Kahle, D. Kloepfel, R. Seifert, J. Hein, and M. C. Kaluza, "Measurement of temperature-dependent absorption and emission spectra of Yb:YAG, Yb:LuAG, and Yb:CaF_2 between 20°C and 200°C and predictions on their influence on laser performance," *JOSA B* **29**(9), pp. 2493–2502, 2012.
4. M. Stehlík, J. Šulc, P. Boháček, H. Jelínková, K. Nejezchleb, B. Trunda, L. Havlák, M. Nikl, and K. Jurek, "Wavelength tunability of laser based on Yb-doped GGAG crystal," *Laser Physics* **28**(10), p. 105802, 2018.
5. B. M. Walsh, J. M. McMahon, W. C. Edwards, N. P. Barnes, R. W. Equall, and R. L. Hutcheson, "Spectroscopic characterization of Nd:Y_2O_3: application toward a differential absorption lidar system for remote sensing of ozone," *JOSA B* **19**(12), pp. 2893–2903, 2002.
6. F. Chen, J. Sun, R. Yan, and X. Yu, "Reabsorption cross section of Nd^{3+}-doped quasi-three-level lasers," *Scientific reports* **9**(1), p. 5620, 2019.
7. T. Fan and R. Byer, "Modeling and cw operation of a quasi-three-level 946 nm Nd:YAG laser," *IEEE Journal of Quantum Electronics* **23**(5), pp. 605–612, 1987.

Downloaded From: https://www.spiedigitallibrary.org/conference-proceedings-of-spie on 05 Oct 2020
Terms of Use: https://www.spiedigitallibrary.org/terms-of-use

8. W. Risk, "Modeling of longitudinally pumped solid-state lasers exhibiting reabsorption losses," *JOSA B* **5**(7), pp. 1412–1423, 1988.
9. A. Schlatter, L. Krainer, M. Golling, R. Paschotta, D. Ebling, and U. Keller, "Passively mode-locked 914 nm Nd:YVO_4 laser," *Optics letters* **30**(1), pp. 44–46, 2005.
10. Y. Lü, J. Xia, X. Zhang, Z. Liu, and J. Chen, "Dual-wavelength laser operation at 1064 and 914 nm in two Nd:YVO_4 crystals," *Laser Physics* **20**(4), pp. 737–739, 2010.
11. P. Jiang, X. Ding, Q. Sheng, B. Li, X. Yu, G. Zhang, B. Sun, L. Wu, J. Liu, W. Zhang, *et al.*, "Efficient 914 nm Nd:YVO_4 laser under double-end polarized pumping," *Applied optics* **55**(5), pp. 1072–1075, 2016.
12. T. Taira, A. Mukai, Y. Nozawa, and T. Kobayashi, "Single-mode oscillation of laser-diode-pumped Nd:YVO_4 microchip lasers," *Optics letters* **16**(24), pp. 1955–1957, 1991.
13. Y. Sato, T. Taira, N. Pavel, and V. Lupei, "Laser operation with near quantum-defect slope efficiency in Nd:YVO_4 under direct pumping into the emitting level," *Applied physics letters* **82**(6), pp. 844–846, 2003.
14. Y. Sato and T. Taira, "The studies of thermal conductivity in $GdVO_4$, YVO_4 , and $Y_3Al_5O_{12}$ measured by quasi-one-dimensional flash method," *Optics express* **14**(22), pp. 10528–10536, 2006.
15. L. McDonagh, R. Wallenstein, R. Knappe, and A. Nebel, "High-efficiency 60 W TEM00 Nd:YVO_4 oscillator pumped at 888 nm," *Optics letters* **31**(22), pp. 3297–3299, 2006.
16. S. Zhao, X. Zhang, J. Zheng, L. Chen, Z. Cheng, and H. Cheng, "Passively Q-switched self-frequency-doubling Nd^{3+}:$GdCa_4O(BO_3)_3$ laser with GaAs saturable absorber," *Optical Engineering-Bellingham-International Soceiety For Optical Engineering* **41**(3), pp. 559–560, 2002.
17. Z. Li, Z. Xiong, N. Moore, G. Lim, W. Huang, and D. Huang, "Pulse width reduction in AO Q-switched diode-pumped Nd:YVO_4 laser with GaAs coupler," *Optics communications* **237**(4-6), pp. 411–416, 2004.
18. X. Yu, R. Yan, X. Li, Y. Ma, D. Chen, and J. Yu, "High power 2 MHz passively Q-switched nanosecond Nd:YVO_4/Cr^{4+}:YAG 914 nm laser," *Applied optics* **51**(14), pp. 2728–2732, 2012.
19. M.-D. Wei, C.-H. Chen, and K.-C. Tu, "Spatial and temporal instabilities in a passively Q-switched Nd:YAG laser with a Cr^{4+}:YAG saturable absorber," *Optics express* **12**(17), pp. 3972–3980, 2004.
20. M.-D. Wei, C.-C. Cheng, and S.-S. Wu, "Instability and satellite pulse of passively Q-switching Nd:$LuVO_4$ laser with Cr^{4+}:YAG saturable absorber," *Optics Communications* **281**(13), pp. 3527–3531, 2008.
21. A. Tucker, M. Birnbaum, C. Fincher, and J. Erler, "Stimulated-emission cross section at 1064 and 1342 nm in Nd:YVO_4," *Journal of Applied Physics* **48**(12), pp. 4907–4911, 1977.
22. S. E. Pourmand, N. Bidin, and H. Bakhtiar, "Effects of temperature and input energy on a quasi-three-level emission cross section of Nd^{3+}:YAG pumped by a flashlamp," *Chinese Physics B* **21**(9), p. 094214, 2012.
23. G. Turri, H. P. Jenssen, F. Cornacchia, M. Tonelli, and M. Bass, "Temperature-dependent stimulated emission cross section in Nd^{3+}:YVO_4 crystals," *JOSA B* **26**(11), pp. 2084–2088, 2009.
24. X. Délen, F. Balembois, and P. Georges, "Temperature dependence of the emission cross section of Nd:YVO_4 around 1064 nm and consequences on laser operation," *JOSA B* **28**(5), pp. 972–976, 2011.
25. G. Krishnan, N. Bidin, M. Ahmad, and M. Abdullah, "Stimulated emission cross section at various temperatures based on laser performance," *Laser Physics Letters* **12**(10), p. 105001, 2015.
26. Y. Sato and T. Taira, "Temperature dependencies of stimulated emission cross section for Nd-doped solid-state laser materials," *Optical Materials Express* **2**(8), pp. 1076–1087, 2012.
27. M. Bass, L. S. Weichman, S. Vigil, and B. K. Brickeen, "The temperature dependence of Nd^{3+}-doped solid-state lasers," *IEEE journal of quantum electronics* **39**(6), pp. 741–748, 2003.

Downloaded From: https://www.spiedigitallibrary.org/conference-proceedings-of-spie on 05 Oct 2020
Terms of Use: https://www.spiedigitallibrary.org/terms-of-use